

Optical Observations of Lightning from a High-Altitude Airplane

H. J. CHRISTIAN

Earth Science and Applications Division, Marshall Space Flight Center, Huntsville, AL 35812

S. J. GOODMAN

Universities Space Research Association, Marshall Space Flight Center, Huntsville, AL 35812

(Manuscript received 11 November 1986, in final form 13 May 1987)

ABSTRACT

Lightning has been observed from above cloud top by using satellites, balloons, rockets, and high-altitude airplanes, each of which provides a unique perspective and holds the potential for gaining new understanding of lightning phenomena. During the 1980s extensive optical observations of lightning have been made from a NASA U-2 airplane with a goal toward placing a lightning sensor in geostationary orbit. Analysis of these U-2 measurements suggest that most of the light generated within a cloud escapes, and that the optical energy of lightning measured from above clouds is not significantly different than the measurements made from below of discharges to ground. Near-infrared optical measurements were made of nearly 1300 optical pulses produced by 79 lightning flashes. The median source estimate of peak flash radiance is approximately 10^8 W with a dynamic range of less than three orders of magnitude. Of these 79 flashes, 90 percent produced peak radiant energy densities of $4.7 \mu\text{J m}^{-2} \text{sr}^{-1}$ or greater, relative to the full field of view of the instrument. The median pulse rise time and full width at half maximum are 240 and 370 μs , respectively. We interpret these slow optical rise times and broad pulse widths as primarily a result of multiple scattering within the cloud. The spectral characteristics in the near-infrared of the neutral emission lines observed from above clouds are found to be very similar to ground-based measurements.

1. Introduction

Lightning has been observed from above clouds using both radio frequency (rf) and optical sensors installed on airplanes (e.g., Christian et al., 1983; Brook et al., 1985), balloons (e.g., Holzworth and Chiu, 1982) and satellites (e.g., Turman, 1979). Each platform produces a different perspective of lightning activity and new insights can be gained from each approach.

While this paper discusses observations of lightning made from a high-altitude airplane, a major motivation comes from the desire to place a sensor in geostationary orbit that is capable of continuously mapping lightning discharges during daytime and nighttime with a high spatial resolution. With this instrument, scientists will for the first time be able to study the electrosphere from scales on the order of the earth's diameter down to the size of individual thunderstorms. They will be able to study both spatial and temporal evolution of lightning activity on a continuous basis and relate the lightning measurements to other observables such as cloud images, radar returns, and the standard meteorological variables on both the synoptic and mesoscale. The ability to study lightning activity in continental storms will be improved because a lightning mapper will detect all types of lightning phenomena, will provide near-uniform spatial coverage and detection efficiency, and will disseminate the information in a readily usable

form. However, in order to develop such a sensor it is essential that we understand the optical characteristics of lightning as seen from above clouds. This paper presents the first quantitative above-cloud optical measurements and provides a much needed contribution toward the design of a satellite lightning sensor.

As a result of their close proximity to cloud tops, high-flying aircraft make excellent platforms from which to make detailed studies of lightning characteristics. In addition, airplanes can be vectored to any specific region of a cloud to facilitate coordinated studies from above and below the same storms. While extensive ground-based optical measurements of lightning have been made, they have tended to concentrate on cloud-to-ground lightning with very little study of intracloud activity. In addition, optical measurements of in-cloud lightning are strongly affected by light scattering by cloud particles and by variable-source geometries. For these reasons, extrapolations of above-cloud optical lightning characteristics from existing ground-based measurements are a fruitless pursuit.

2. Optical instrumentation

In recent years, a NASA U-2 airplane carrying an instrument package for studying the electrical and optical characteristics of lightning has been flown over a

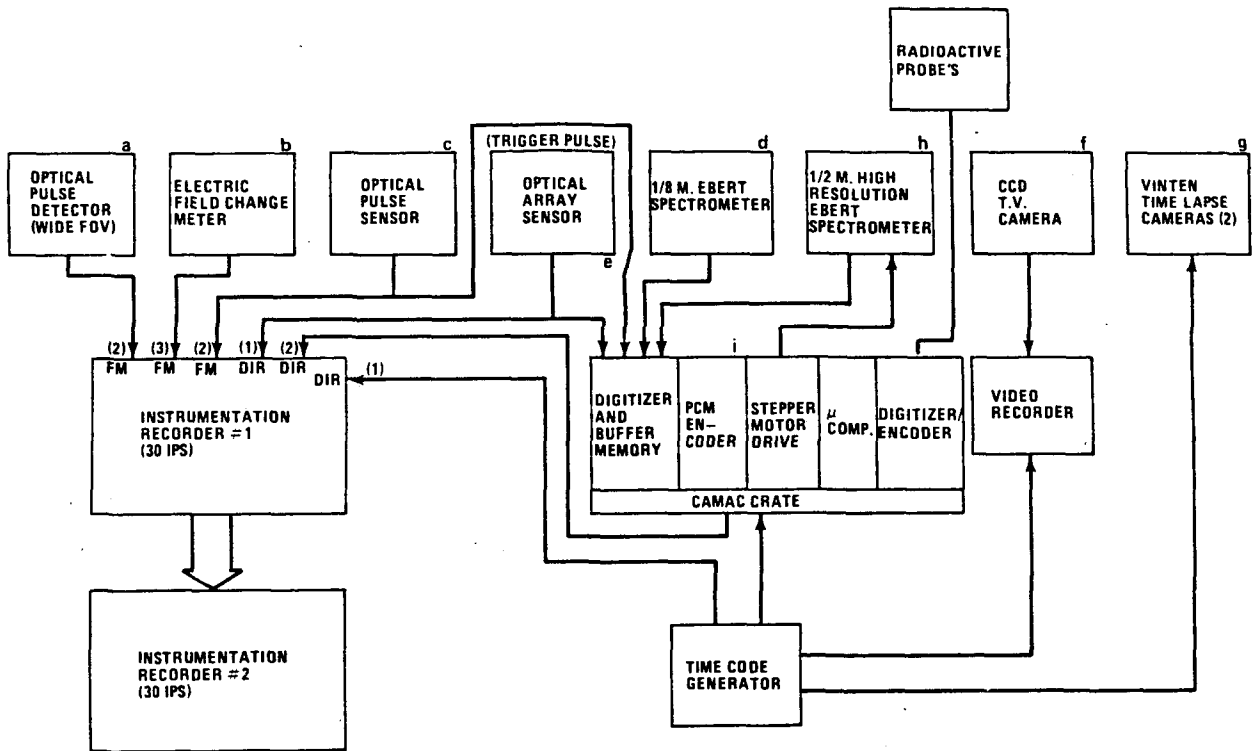


FIG. 1. Block diagram of U-2 aircraft lightning instrumentation.

variety of thunderstorms (Christian et al., 1983). The package utilizes an array of sensors encompassing large temporal, spatial and spectral ranges and resolutions. A block diagram of the instrumentation package and a photograph of the instrument pallet is shown in Figs. 1 and 2, respectively. Each instrument complements one another by cascading temporal resolution (1–10 s), spatial resolution (1 m–5 km) and spectral resolutions (5–300 nm) in such a manner that the required

ranges are partitioned between the instruments. Details of only the optical pulse sensor (OPS) and broadband spectrometer (BBS) will be discussed here, since they are the primary sensors used to acquire the data discussed in this paper.

a. Optical pulse sensor

The optical pulse sensor (OPS) consists of a photodiode at the focus of a wide angle (60°) field-of-view lens (Fig. 3). An interference filter is installed at the front of the lens prior to each flight and cannot be changed during the flight. A filter is usually selected that has a bandpass optimized to pass one specific lightning spectral emission line. During most flights either a 777.4 nm OI(1) (neutral atomic oxygen line) or 868.3 nm NI(1) (neutral atomic nitrogen line) filter has been used.

The output of the photodiode is amplified by a current amplifier followed by a high-pass filter and additional amplification. The filter pass band is set so that rapidly varying signals due to lightning are passed and slowly varying signals (i.e., sunlight reflecting from cloud tops) are strongly attenuated. Thus the output from the OPS contains only lightning signals from an ac-coupled sensor. The OPS data are stored at different gains on two WBII FM channels of an instrumentation recorder running at 76 cm s^{-1} (30 ips). This arrangement provides a recorder limited-frequency response

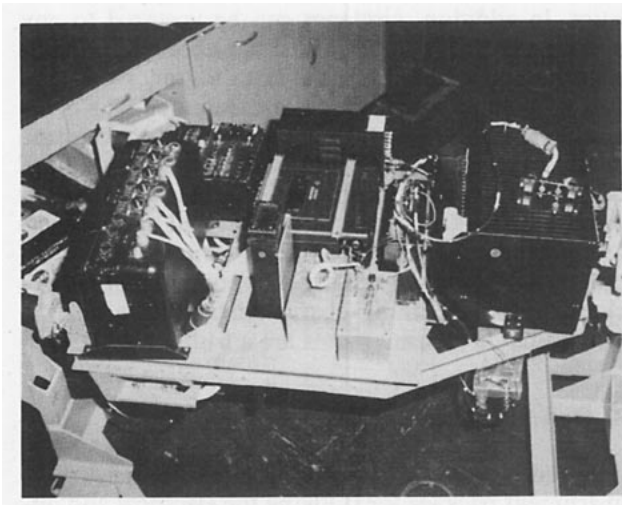


FIG. 2. Photograph of the U-2 instrumentation pallet.

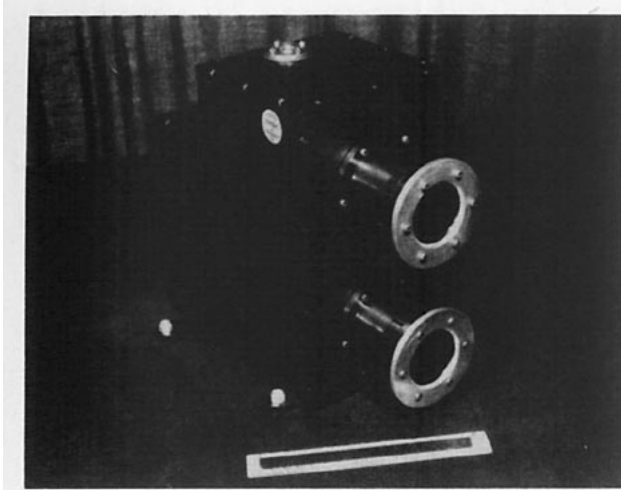


FIG. 3. Photograph of the optical pulse sensor.

of 125 kHz and, thus, an effective rise time limit of better than $4 \mu\text{s}$. The OPS is calibrated against a National Bureau of Standards referenced standard lamp so that absolute radiance values can be determined. A separate calibration is performed on each interference filter and each f/stop setting of the sensor's lens.

The primary use of the OPS is to determine time-resolved lightning optical pulse characteristics. The data contain information on absolute radiant-energy density, peak optical-power density, and pulse rise times, widths, amplitudes and durations. The OPS is not an imaging sensor; information on the spatial extent of an event is provided by time lapse and TV cameras.

b. Broadband spectrometer

The broadband spectrometer (BBS) consists of a $\frac{1}{8}$ -m focal length Ebert spectrometer with an expanded exit slit (Fig. 4). A fiber optic plug couples light from the exit slit to a microchannel plate image intensifier that provides an effective optical gain of more than 10 000 to 1. The light emitted from the intensifier's photoanode is detected with a 512 element S-series linear Reticon photodiode array. The diodes are spaced on $25 \mu\text{m}$ centers along the dispersion axis. With a 300 line per millimeter grating, the spectrometer dispersion is approximately 25 nm mm^{-1} . The resulting theoretical spectral resolution of 0.6 nm is reduced to 1.2 nm by a $50 \mu\text{m}$ wide entrance slit. Thus, the entrance slit is imaged across two photodiodes. In addition, the modulation transfer function of the image intensifier and the custom-expanded exit slit on the Ebert spectrometer both contribute toward degrading the overall spectral resolution to approximately 2 nm .

Each photodiode integrates its incident light for 5 ms before being read out. The output of each photodiode is multiplexed into a serial data stream with each diode accessed into the stream in a sequential manner.

Thus, even though the total frame time to read out each complete spectrum is 5 ms, the sequential multiplexing causes a diode-to-diode time skew to occur. The effects of this skew are discussed in the next section.

After amplification, the BBS data stream is split and stored in both analog and digital formats as shown in Fig. 1. The analog signal is stored on a direct channel of the instrumentation recorder and serves both as a backup for the digital signal and to fill in for the digital dead time that occurs while the buffer memories of the transient recorders are formatted and transferred to the instrumentation recorder. The transient recorder used for the spectrometers consists of a 10-bit digitizer and a 128K word buffer memory. Data are continuously digitized until an OPS signal above a preset level triggers the system. At that point, the digitizer continues for a user-selectable number of samples and then switches to its readout mode. During the readout period the spectrometer data are formatted into a 400 kHz pulse code-modulated bit stream and recorded on a direct channel of the instrumentation recorder. The total readout time for both transient recorders is less than 5 s. This is the dead period during which no new lightning signals can be digitized. Like the OPS, the BBS was calibrated against a standard lamp for absolute radiance determination. A scanning dual monochromator was used to determine the spectral response of the instrument.

3. Observations

The types of questions that will be addressed in this section concern such simple concepts as: How bright is lightning when viewed from above? What does it look like? What are the time-resolved characteristics of the emissions? What are the spectral and spatial characteristics? While these questions may seem rather basic, it must be remembered that most previous optical lightning measurements have been made of the

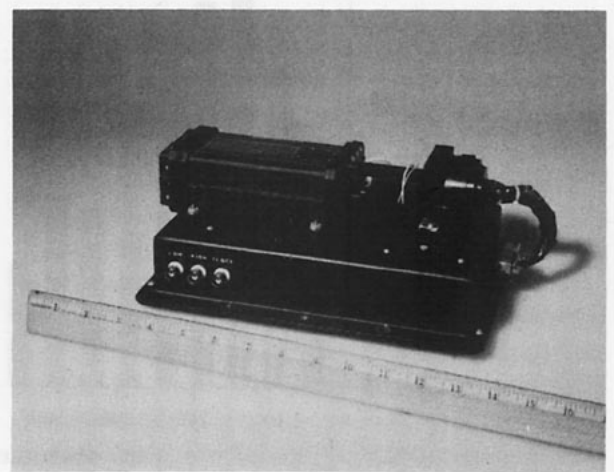


FIG. 4. Photograph of the broadband spectrometer.



FIG. 5. Vinten camera photograph of lightning flash at 0342:28 UTC 4 June 1983.

unobstructed channel of cloud-to-ground flashes. The determinations of optical power, pulse rise times, spectrum, etc. have been based on that portion of the channel (which is nearly a linear line source) that occurs below cloud base.

From the top, we see a much different picture. As shown in Fig. 5, a lightning flash generally appears as diffuse illumination radiating from the top of a cloud. In actuality, the light source can be anywhere within the cloud. What is seen at the top are lightning emis-

sions that have been modified by scattering through an optically thick medium, i.e., the cloud. Thomason and Krider (1982) developed a Monte Carlo radiative transfer model in order to study the effects of a cloud on optical lightning emissions. Their results, based on the facts that at optical wavelengths the cloud is basically a conservative scatterer (there is very little absorption), suggest that the lightning illumination at the top surface of a cloud should be on the same order as that seen from below. Further, their calculations predict that because the light must often radiate through hundreds of optical depths of cloud, a typical optical pulse should have a significantly longer rise time and broader half-width than the optical pulse from an unobscured return stroke one would measure from ground.

Figures 6 and 7 show the 10%–90% rise time and 50% pulse-width distributions from 79 lightning flashes (over 1200 pulses) measured by the OPS from a U-2 airplane. The medians for these distributions are 240 and 370 μ s, respectively. A sketch of the typical optical pulse shape is presented in Fig. 8. In comparison, Guo and Krider (1982) measured typical return-stroke pulse shapes with a ground-based photodetector and found the linear portion of the return-stroke rise times (extrapolated to a 10%–90% value) were on the order of 25 μ s with median pulse widths of 157 μ s.

On ground strokes, it is generally believed that pulse rise times are dominated by the vertical propagation velocity of the return stroke, whereas the pulse widths are a function of the discharge process. The difference between mean ground-stroke pulse widths and the mean optical pulse widths observed from above cloud top is approximately 210 μ s. In addition, the above-cloud measurement of rise times are found to be 215 μ s slower. One would expect that the above-cloud

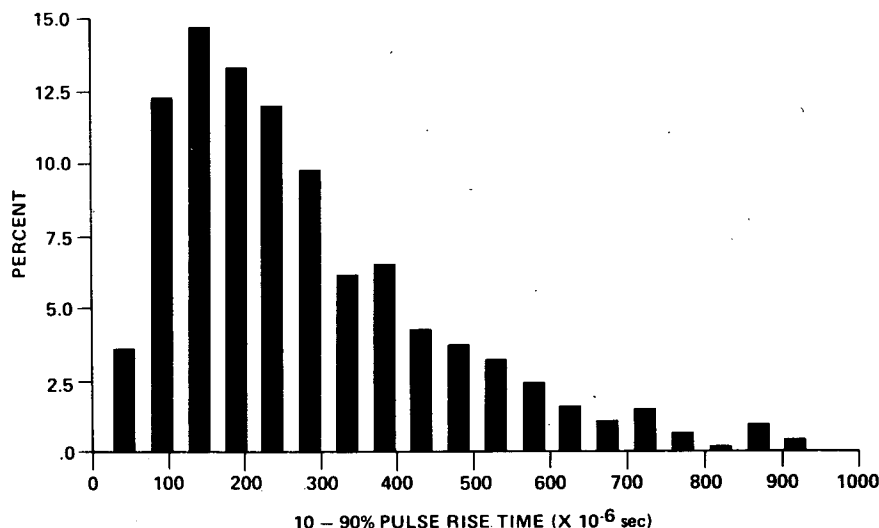


FIG. 6. 10%–90% pulse-rise time distribution for 1272 optical pulses.

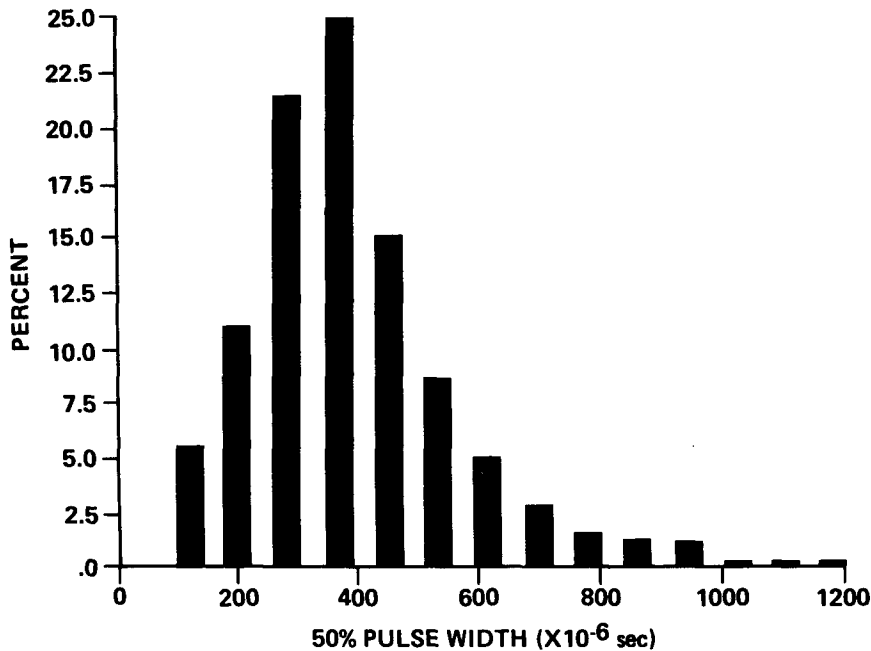


FIG. 7. 50% (FWHM) pulse-width distribution for 1323 optical pulses.

measured rise times would be strongly affected by geometric growth of the lightning channel and by multiple scattering-produced time delays, whereas the broadened pulse widths should be primarily influenced by multiple scattering, and thus have a smaller delay. Since both rise times and pulse widths are affected by similar time differences, we suspect that the enhancement of the photon optical paths by multiple scattering within the cloud, rather than geometric growth, accounts for most of the time delay and time broadening of the light signal. This speculation, naturally, requires detailed evaluation using computer modeling.

In order for geometric growth not to make a significant contribution to the pulse rise times, the streamer process that generates the optical emissions must either

be very fast or the emissions must be generated over a small distance. Ogawa and Brook (1964) studied both the electric field and optical characteristics of intracloud processes. They determined that short-duration, bright luminous events were associated with K changes. Further, they estimated a K-change channel length at 1.3 km and a propagation velocity of $1.3 \times 10^6 \text{ m s}^{-1}$. Most investigators measuring recoil-streamer propagation velocities report speeds greater than 10^6 m s^{-1} , with Proctor (1981) finding speeds that ranged from 2.5×10^6 to $4.4 \times 10^7 \text{ m s}^{-1}$. These results support the assertion that the bright optical emissions observed from above cloud top are produced by fast streamers (K-changes), with velocities on the order of Proctor's measurements.

Following the calculations of Thomason and Krider (1982), we find that the mean time delay of $210 \mu\text{s}$ (or 53 ns per optical path unit) corresponds to a mean optical path of 4000 for a cloud composed of $10 \mu\text{m}$ drops and having a mean free path of 16 m. This corresponds to a point source 500 optical depths below the cloud top or, equivalently, 8 km for their model cloud. That is, it appears from the degree of pulse delay and time broadening that the lightning source is typically 8 km below cloud top, which roughly corresponds to the optical center of the large midwestern storms we have been studying.

Distributions of peak radiance and peak radiant energy densities are shown in Figs. 9 and 10, respectively. These measurements were obtained during U-2 storm overflights and were made using a 868.3 nm [NI(1)] interference filter, and thus reflect the optical output

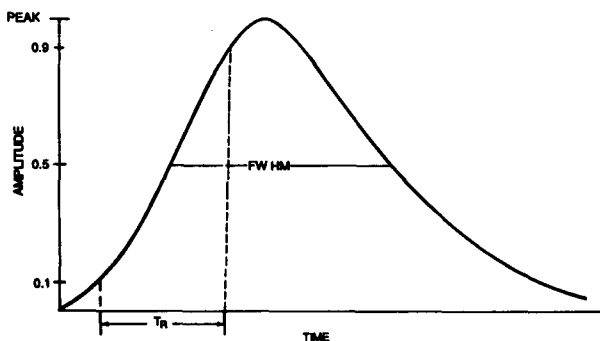


FIG. 8. High temporal resolution sketch of the typical optical pulse waveform produced by lightning. T_R is the 10%-90% rise time and FWHM is the pulse width at half maximum (or 3 dB width).

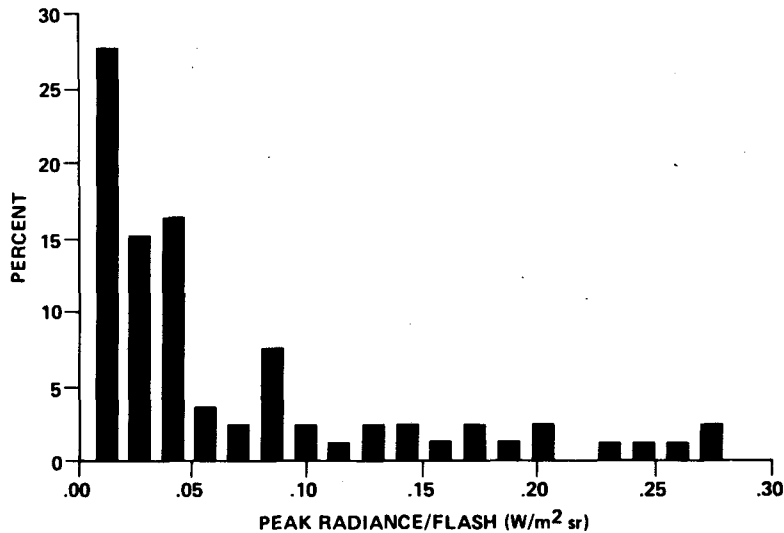


FIG. 9. Peak radiance per flash distribution based on 79 flashes.

from a single emission line. In addition, the output from only the most intense pulse of each lightning flash is contained in these distributions. This selection approach is similar to plotting only the output from the first (and typically the most intense) return stroke of a cloud-to-ground flash (Barasch, 1970) and is used to facilitate comparisons between above-cloud and below-cloud measurements. An additional reason for interest in the strongest optical pulse occurring during a particular flash is that the strongest pulse determines the threshold detectability for observations from space. Of the 79 flashes observed 90 percent produced peak radiant energy densities of $4.7 \mu\text{J m}^{-2} \text{sr}^{-1}$ or greater.

The number of optical pulses detected from above from a single flash is generally much larger than the

number of return strokes associated with ground flashes. Figure 11 shows a pulse-per-flash distribution with a mean of 12 optical pulses per lightning flash. Events containing in excess of 40 pulses are not uncommon. Interpulse intervals are often 10 ms as opposed to return-stroke intervals of 30–40 ms. While the lightning optical emissions are generally made up of many discrete pulses, the total optical output of a flash tends to be dominated by a few large pulses. This is evident when comparing Fig. 12 showing the radiance distribution of all pulses with Fig. 9 having only the peak radiances per flash plotted. While there is a large variation in pulse intensity within a flash, Fig. 13 reveals that only a weak correlation exists between pulse width and pulse amplitude. Again, this is probably a

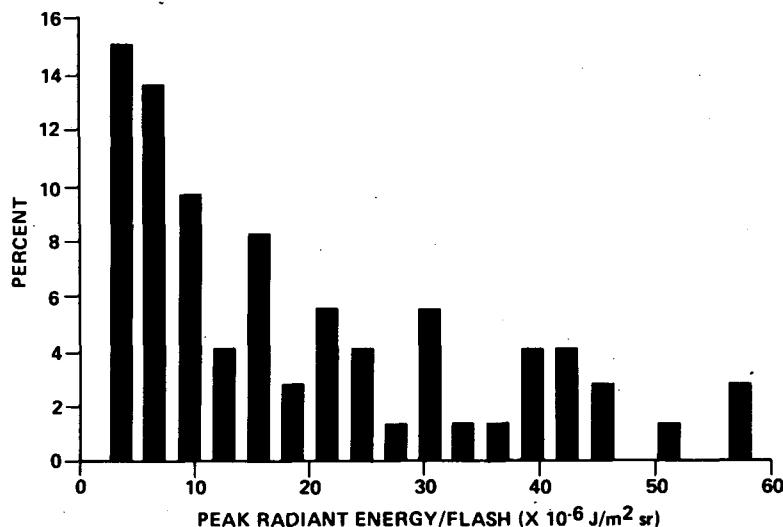


FIG. 10. Peak radiant energy per flash distribution based on 73 flashes.

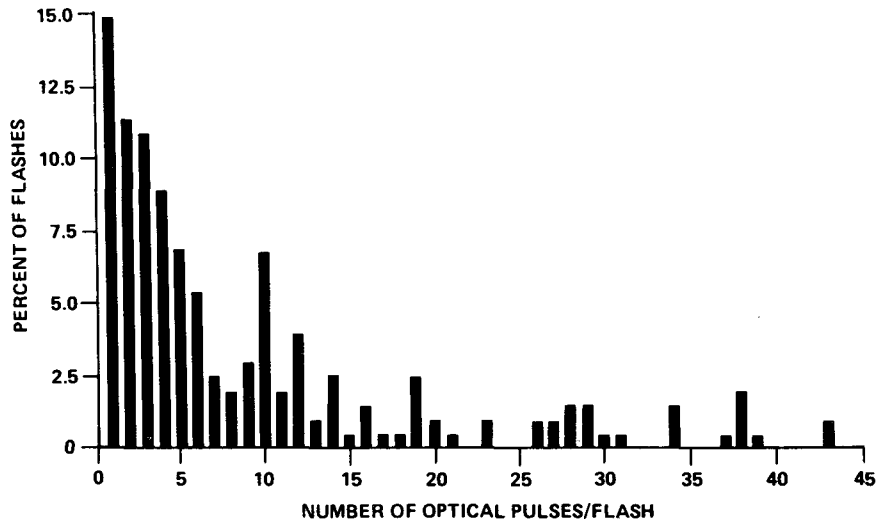


FIG. 11. Distribution of the number of optical pulses in 125 flashes.

consequence of multiple scattering effects dominating the pulse structure. There do not seem to be major differences in pulse shapes between cloud to ground or intracloud processes, nor are there major differences in radiances produced by these processes, with the possible exception that return strokes seem to seldom produce the truly weak optical pulses. (The weak optical return-stroke pulses seem to be a result of events occurring almost completely outside the OPS field of view).

4. Discussion

A series of assumptions are required in order to compare the total optical power measured from above

clouds with ground-based measurements of return strokes. First, most ground measurements have been made with wide-band sensors that detected the lightning output in the visible and near-infrared, whereas the U-2 OPS measurements are generally confined to a single emission line. Measurements by Orville (private communication) suggest that 5%–10% of the optical energy is contained in the NI (868.3 nm) line set. For this comparison, the upper limit of 10% is assumed. If we further assume that the optical source region (the lightning channel) is centered 8 km below cloud top and that the cloud top acts like a Lambertian surface, then a rough estimate can be made of the total source optical power from the U-2 measurements.

A cumulative distribution of U-2 peak power data

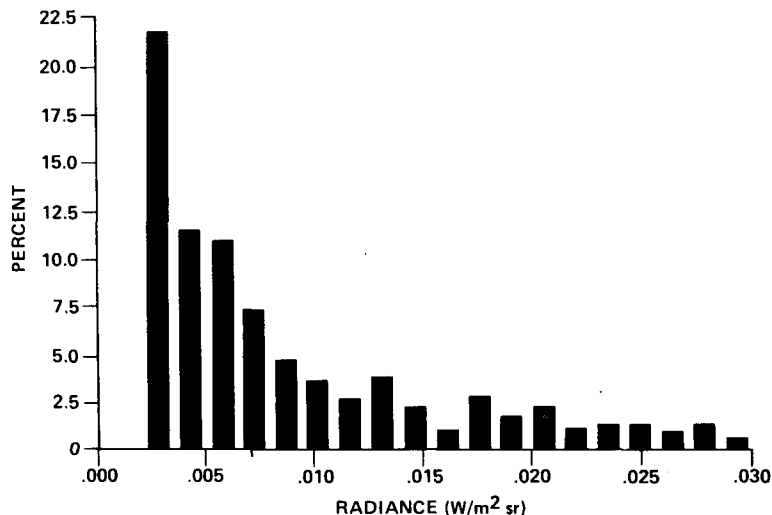


FIG. 12. Distribution of the radiance for 1272 pulses occurring in 79 flashes.

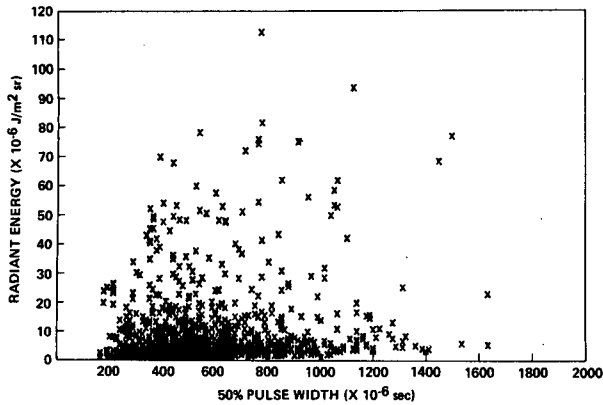


FIG. 13. Scatter diagram of radiant energy versus 50% pulse width.

is compared with the results of Guo and Krider (1982) and Turman (1978) in Fig. 14. Note that the U-2 based measurements closely resemble the Guo-Krider distribution, and when cumulative total energy values (Fig. 15) are compared, time-broadened U-2 measurements actually exceed the Guo-Krider ground-based measurements for strong events. We also believe that the lower end of the U-2 peak power curve presents underestimated values. With the U-2 flying at 20 km and cloud tops at 15–17 km, the instrument field of view is generally much smaller than the illuminated cloud-top area. This produces a fringing effect, with most of the detected lightnings centered outside the OPS field of view. As a consequence, the weaker events tend to correlate with underfilled fringe events, and the low

end of the cumulative distribution is distorted. On average, approximately 60%–65% of the total OPS field of view is fully illuminated.

Figure 16 shows the spectrum of an intracloud event obtained with the broadband spectrometer (BBS). Spectral range of this instrument at the time the data were acquired was from below 600 to almost 900 nm. In this spectral region, dominated by neutral nitrogen and oxygen emission lines, observations from above reveal spectra that are very similar to ground-based measurements of cloud-to-ground flashes (see Orville and Henderson, 1984).

The time-resolved optical waveform for that portion of the lightning event that produced the spectrum in Fig. 16 is shown in Fig. 17. Because of the close temporal spacing of pulses A, B and C and because these pulses occur in the middle of the spectral frames (each diode integrates light for 5 ms, but the readout runs continuously in a sequential fashion) it is necessary to sum over three successive spectral frames in order to remove the effects of readout-generated time skew from the spectral data. Thus, the spectrum shown in Fig. 16 is recorded over a 15 ms interval that contains the three optical pulses.

The optical data in Fig. 17 are obtained with the OPS using a 50 nm-wide interference filter centered near 868.3 nm. Because of the width of this filter, all three lines that comprise the 868.3 nm line set (Salanave, 1980) are passed. In order to compare the pulse data with the spectral data, one must integrate and sum pulses A, B and C, and then compare this value with the spectral signal integrated over the NI(1) signal.

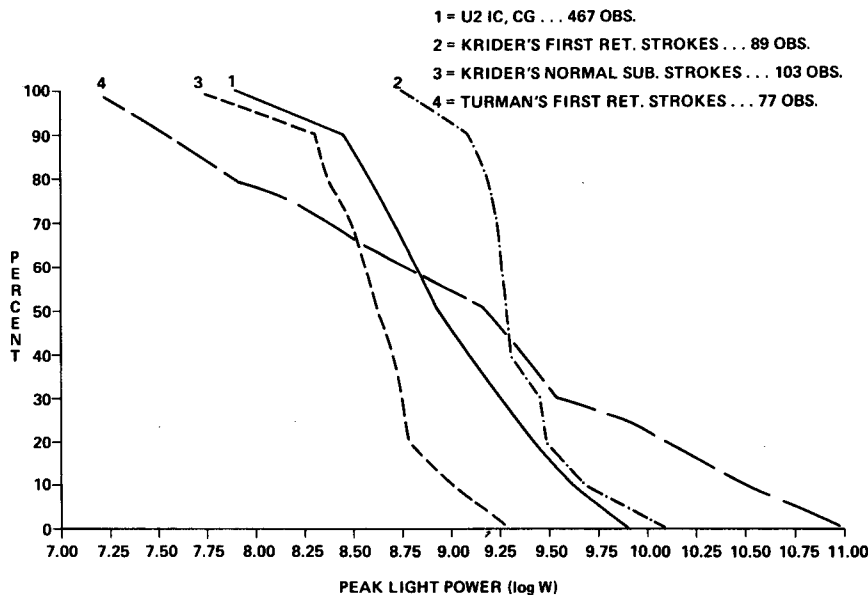


FIG. 14. Cumulative distributions of peak light power (radiance) from 1) U-2 measurements, 2) Guo and Krider's (1982) first strokes, 3) Guo and Krider's subsequent strokes and 4) Turman's (1978) first strokes.

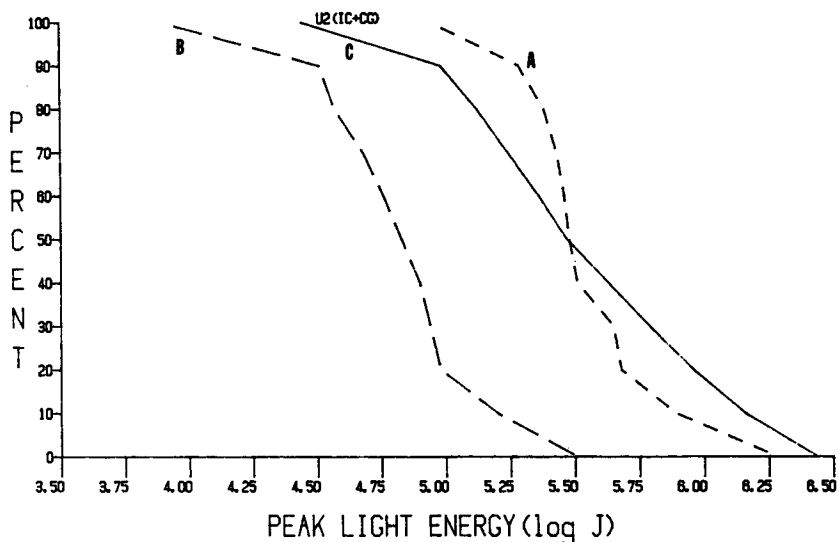


FIG. 15. Cumulative distributions of peak light energy from (a) Guo and Krider's (1982) first strokes, (b) Guo and Krider's subsequent strokes and (c) U-2 measurements.

The total radiant energy density in the three pulses, as measured with the OPS is $465 \mu\text{J m}^{-2} \text{sr}^{-1}$. The radiant energy density of the NI(1) line measured with the BBS is $1150 \mu\text{J m}^{-2} \text{sr}^{-1}$.

Figure 18 is a picture of this same lightning flash taken through a 868.3 nm filter with a CCD TV camera. While the fields of view of the OPS and TV camera are similar (60°), the spectrometer field of view is much smaller (6°). The field of view of the spectrometer is

marked in Fig. 18 and is shown to be fully illuminated by the lightning. The field of view of the OPS, on the other hand, is only about 40% illuminated. If one corrects for this underfilling of the field of view, then the actual radiant energy density of the illuminated area viewed by the OPS becomes $1164 \mu\text{J m}^{-2} \text{sr}^{-1}$, in good agreement with the spectrometer measurement.

It is very difficult to quantitatively compare the spectral radiance measurements made from above

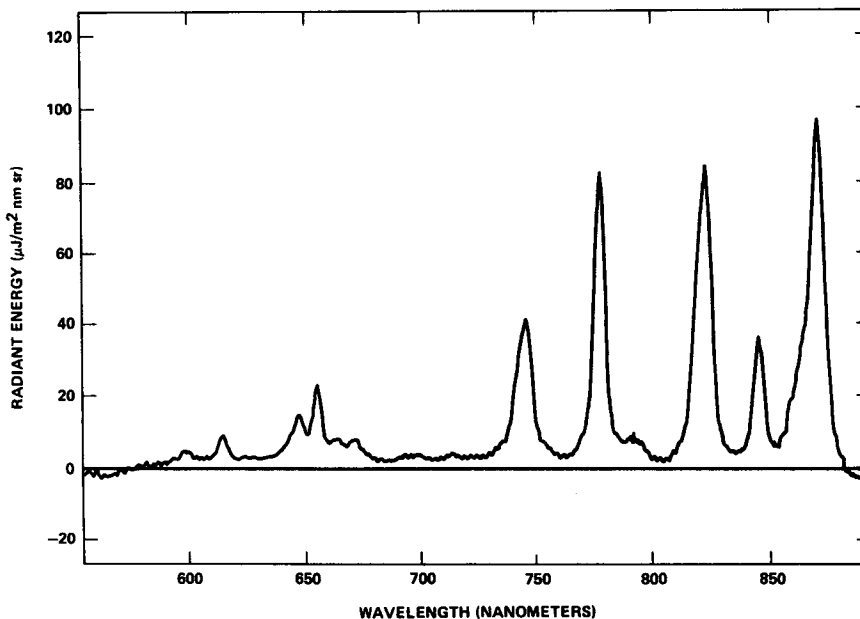


FIG. 16. Absolute spectral radiant energy density as a function of wavelength received by the spectrometer over a 15 ms interval.

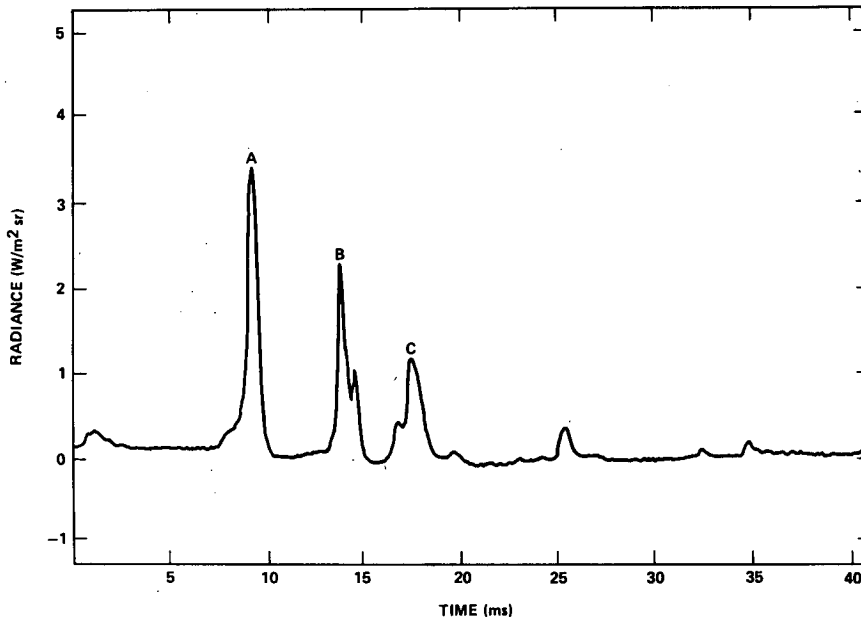


FIG. 17. Time-resolved optical pulse waveforms at 868.3 nm covering the time interval of the spectrum in Fig. 16.

cloud top with the ground-based irradiance measurements of Orville and Henderson (1984) because of significant differences between the signal sources. Assuming that the cloud top forms a Lambertian surface, then as long as the lightning-illuminated area fully fills the spectrometer field of view, the irradiance measurement at the spectrometer can be immediately related to the cloud-top radiance. On the other hand, the Orville and Henderson measurements were made from cloud-to-ground flashes which strongly underfill the spectrometer field of view. Thus, it is very difficult to relate their

irradiance measurements at the spectrometer to the lightning channel source strength.

Barasch (1970) has made spectral-intensity measurements at a total of five wavelengths and attempted to calculate source strengths. One of his filters was centered on the neutral atomic nitrogen line NI(2) at 822.3 nm, one of the stronger lines, as seen from the U-2. His calculations indicate average return-stroke peak radiated power in the NI(2) line of 10^8 W, which compares favorably with U-2 estimated equivalent source powers of just under 10^8 W.

5. Conclusions

Optical sensors have been developed for studying the temporal and spatial characteristics of lightning from above cloud tops. Such measurements present a different perspective to the investigator, providing information from the whole volume of cloud rather than from just the lowest portion of return stroke channels to ground. In addition, these measurements have been invaluable for system design and parametric trade-off studies that are leading to the development of a space-based optical sensor proposed for geostationary orbit (Norwood, 1983; Eaton et al., 1983). This sensor, known as the "lightning mapper", is being designed to detect and locate both intracloud and cloud-to-ground lightning over large areas of the earth's surface, mark their time of occurrence, and measure the radiant energy of each discharge. The sensor is expected to fly on one of the GOES-Next series of satellites in the early 1990 time frame.

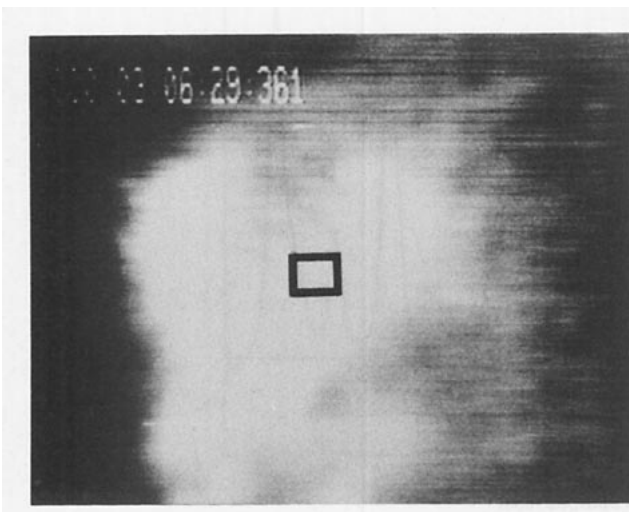


FIG. 18. Area imaged by spectrometer superimposed on CCD TV picture of the flash described in Figs. 16 and 17.

Basic conclusions that can be drawn from the present set of measurements include: 1) the optical energy of both cloud-to-ground and intracloud lightning measured from above cloud top is not significantly different from measurements made of ground discharges beneath clouds; 2) the optical rise times at cloud top are slower and pulse widths are broader, primarily as a result of multiple scattering within the cloud; and 3) the spectral characteristics of the neutral-emission lines at infrared wavelengths are similar to previously made ground-based measurements. These observations further support the assumption that a cloud is an optically thick, conservative scatterer.

Acknowledgments. We wish to thank R. L. Frost for calibration and operation of the U-2 optical sensors and for acquiring the data. This work was partially sponsored by the Universities Space Research Association under NASA Contract NAS8-34748.

REFERENCES

- Barasch, G. E., 1970: Spectral intensities emitted by lightning discharges. *J. Geophys. Res.*, **75**, 1049.
- Brook, M., C. Rhodes, O. H. Vaughan, Jr., R. E. Orville and B. Vonnegut, 1985: Nighttime observations of thunderstorm electrical activity from a high-altitude airplane. *J. Geophys. Res.*, **90**, 6111-6120.
- Christian, H. J., R. L. Frost, P. H. Gillaspay, S. J. Goodman, O. H. Vaughan, M. Brook, B. Vonnegut and R. E. Orville, 1983: Observations of optical lightning emissions from above thunderstorms using U-2 aircraft. *Bull. Amer. Meteor. Soc.*, **64**, 2, 120.
- Eaton, L. R., C. W. Poom, J. C. Shelton, N. P. Lavery and R. D. Cook, 1983: Lightning mapper sensor design study. NASA CR-170909, Marshall Space Flight Center.
- Guo, C., and E. P. Krider, 1982: The optical and radiation field signatures produced by lightning return strokes. *J. Geophys. Res.*, **87**, 8913.
- Holzworth, R. H., and Y. T. Chiu, 1982: Sferics in the stratosphere. *CRC Handbook of Atmospheric Vol. II*, H. Volland, Ed., 1-19.
- Norwood, V., 1983: Lightning mapper sensor study. NASA CR-170908, Marshall Space Flight Center.
- Ogawa, T., and M. Brook, 1964: The mechanism of the intracloud lightning discharge. *J. Geophys. Res.*, **69**, 5141.
- Orville, R. E., and R. Henderson, 1984: Absolute spectral irradiance measurements of lightning from 375 to 880 nm. *J. Atmos. Sci.*, **41**, 3180-3187.
- Proctor, D. E., 1981: VHF radio pictures of cloud flashes. *J. Geophys. Res.*, **86**, 4041.
- Salanave, L., 1980: *Lightning and its Spectrum*. University of Arizona Press.
- Thomason, L. W., and E. P. Krider, 1982: The effects of cloud on the light produced by lightning. *J. Atmos. Sci.*, **39**, 2051.
- Turman, B. N., 1978: Analysis of lightning data from the DMSP satellite. *J. Geophys. Res.*, **83**, 5019.
- , 1979: Lightning detection from space. *Amer. Scientist*, May-June, 321.